Arch. Metall. Mater. **71** (2026), 1, 213-223

DOI: https://doi.org/10.24425/amm.2026.157783

RUIXIANG WANG[1], BOHAN WEI[1], QING CHEN[1], KUIFANG ZHANG[2*]

RECOVERY OF YTTRIUM FROM STRONG ACIDIC SULPHATE LEACH SOLUTIONS OF PHOSPHATE ROCK RESOURCES USING A NOVEL ACIDIC PHOSPHORUS EXTRACTANT

A novel acidic phosphorus extractant (NAPE) was utilized to directly extract yttrium from highly acidic sulfate leach solutions derived from phosphate rock resources. The results indicated that the application acidity of NAPE exceeded those of the commonly used phosphate esters (P204, P507 and Cyanex272), and could directly extract yttrium from the strong acidic sulphate leach solutions (pH = 0.33). In batch experiments, 100% of yttrium was extracted from sulfuric solutions with a pH of 0.33 containing 0.203 g/L of yttrium, using a five-stage counter-current extraction process. The organic system consisted of 10% (v/v) NAPE and 5% (v/v) TBP in sulfonated kerosene, with an A/O ratio of 2:1, conducted at a laboratory temperature of 27±1°C over 10 minutes. Additionally, the extraction of other metals (aluminum, magnesium, manganese, and calcium) was minimal, with the exception of iron. Subsequently, 97.7% of the yttrium in the loaded organic phase was selectively stripped using a 1 mol/L H_2SO_4 solution, followed by a 1 mol/L $H_2C_2O_4$ solution to strip the co-extracted iron for recycling purposes. Throughout the entire process, 97.7% of yttrium was recovered and concentrated in the strip liquor to a concentration of 1.5863 g/L. The yttrium in the strip liquor was easily recovered through sodium oxalate precipitation. After roasting, a yttrium oxide product was obtained with impurity elements such as Fe, Al, Mn, Mg, Ca, and P content less than 0.02%.

Keywords: Phosphate rock; Strong acidic Sulphate leach solutions; Yttrium; NAPE; Solvent extraction

1. Introduction

Yttrium is a widely utilized rare earth element that demonstrates exceptional performance in various fields, including metal alloys [1-5], luminescent materials [6-10], laser materials [11-13], high-temperature superconducting materials [14-17], and precision ceramic materials [18-20]. It is also used in high-temperature spray materials, as a diluent for nuclear reactor fuels, as an additive in permanent magnetic materials, and as a getter in the electronics industry [21,22]. The application areas for yttrium continue to expand, and the demand for yttrium is expected to increase significantly in the coming years, making the study of its extraction technology highly significant.

Yttrium is primarily sourced from ionic rare earth ores, with minor contributions from fluorocarbon waste, monazite, and nuclear fission byproducts. Phosphate ores, which are plentiful and frequently contain rare earth elements, including yttrium, are particularly significant. Global phosphate ore reserves are estimated at around 71 billion tons, with an average rare earth content of 0.5%, amounting to approximately 355 million tons of rare earth elements. These rare earths are predominantly found in minerals such as collophane, apatite, and phosphorite, where they replace other elements in the crystal lattice, with yttrium being the most prevalent, often occurring as xenotime [23]. Yttrium in phosphate rock exists as phosphates. The low solubility product constant of yttrium phosphate necessitates high-acid leaching to ensure its dissolution, resulting in highly acidic sulfate leach solutions that are characterized by low yttrium concentration and complex impurities. However, extracting yttrium from these acid leaching solutions of phosphate ores is technically challenging due to current limitations in extraction technology.

The preferred method for separating and recovering yttrium from acid leaching solutions is solvent extraction. Extractants can be categorized based on their properties as follows: (1) Acidic phosphorus-based extractants, such as P204 [24,25], P507 [26-28], Cyanex272 [29,30], and Cyanex302 [31,32]. These extractants offer advantages like low cost, strong extraction capability, and easy stripping. However, commonly

[1] JIANGXI UNIVERSITY OF SCIENCE AND TECHNOLOGY, COLLEGE OF METALLURGICAL ENGINEERING, GANZHOU 341000, CHINA
[2] GANNAN UNIVERSITY OF SCIENCE AND TECHNOLOGY, SCHOOL OF INTELLIGENT MANUFACTURING AND MATERIALS ENGINEERING, GANZHOU KEY LABORATORY OF GREEN EXTRACTION AND HIGH QUALITY UTILIZATION OF REGIONAL CHARACTERISTIC METAL RESOURCES, GANZHOU 341000, CHINA

* Corresponding author: zhang_kui_fang@163.com

used extractants like P204, P507, and Cyanex272 have limited application acidity and average selectivity, making them unsuitable for recovering yttrium from high-acid phosphate ore leaching solutions. (2) Neutral and amine extractants, such as TBP [33,34], P350 [35], N235 [36], Cyanex923, and Cyanex925 [37-39], require yttrium to be extracted into the organic phase as an anion or neutral molecule. The addition of complexing agents during the extraction process significantly increases costs and operational complexity. (3) Carboxylic acid extractants, such as cyclohexane carboxylic acid [40,41], CA-12 [42], and CA-100 [43-45], are effective and selective but suffer from poor stability, emulsification, high losses, and are not suitable for high-acid systems. Furthermore, Singh and collaborators synthesized di-nonylphenyl phosphoric acid (DNPPA) and employed it primarily for the solvent extraction of uranium [46,47]. During uranium extraction, trace rare-earth elements present in the original solution are co-extracted. The synthesized DNPPA consists predominantly of diesters, necessitating the use of the highly toxic phosphorus oxychloride as a phosphate esterification reagent. Thus, its industrial applications are relatively limited. To circumvent this drawback, we prepared NAPE, a monoester-based extractant (nonyl-p-phenyl phosphate), thereby eliminating the need for phosphorus oxychloride. This paper studies the process of recovering yttrium from high-acidity phosphate ore leachate using NAPE, a new type of monoester, and explores the feasibility of its potential industrial applications.

2. Experimental

2.1. Materials

The diluent sulfonated kerosene (technical grade) was obtained from Shanghai Laiyashi Chemical Company. Sulfuric acid (analytical reagent), hydrochloric acid (analytical reagent), nitric acid (analytical reagent), oxalic acid (analytical reagent), and sodium carbonate (analytical reagent) were sourced from Guangzhou Chemical Reagent Factory. The extractant NAPE, with a purity of 89.6%, was synthesized by our research team and primarily consists of nonyl-p-phenyl phosphate. The total impurity content is 10.4%, predominantly unreacted nonylphenol, and its photo and molecular structure are depicted in Fig. 1.

The main composition of sulphate leach solutions of phosphate rock is shown in TABLE 1.

TABLE 1

Chemical compositions of the sulphate leach solutions of phosphate rock

Element	Y	Fe	Al	Ca	Mg	Mn
Concentration (g/L)	0.203	1.75	0.830	0.670	5.40	0.501

2.2. Methods

The single-stage extraction, scrubbing, and stripping tests were conducted by shaking the aqueous and organic solutions together in a 125 mL separating funnel (Tianjin Tianke Glass Company) in an oscillator (Shaoxing Subo Instrument Manufacturing Company) for a specified duration. The acidity of the aqueous solution was adjusted using H_2SO_4 or Na_2CO_3 and measured with a PHSJ-6L digital pH meter. To determine the yttrium extraction distribution isotherms, the sulfate leach solutions and NAPE organic solutions were mixed at A/O ratios of 5:1, 3:1, 2:1, and 1:1. For the yttrium stripping distribution isotherms, the loaded organic solutions were contacted with yttrium strip solution at A/O ratios of 1:1, 1:2, 1:5, and 1:10. To ascertain the iron stripping distribution isotherms, the loaded organic solutions, after yttrium stripping, were contacted with iron strip solution at A/O ratios of 1:1, 1:2, 1:5, and 1:10. The multistage counter-current extraction and stripping tests were performed using multiple 125 mL separating funnels and simulated by the "funnel method" [48]. The changing ratio method [49] was used to draw the isotherms. The number of stages for multistage counter-current extraction and stripping was determined using the McCabe-Thiele graphical analysis method [50]. All shake experiments were conducted at laboratory temperature (27±1°C) for 10 minutes.

The flowchart for the *n*-stage counter-current extraction is depicted in Fig. 2. In the diagram, the first stage functions as the inlet for the aqueous phase and the outlet for the organic phase, with the loaded organic phase E being discharged from this stage. The nth stage serves as the inlet for the organic phase and the outlet for the aqueous phase, with the raffinate R being discharged from this stage.

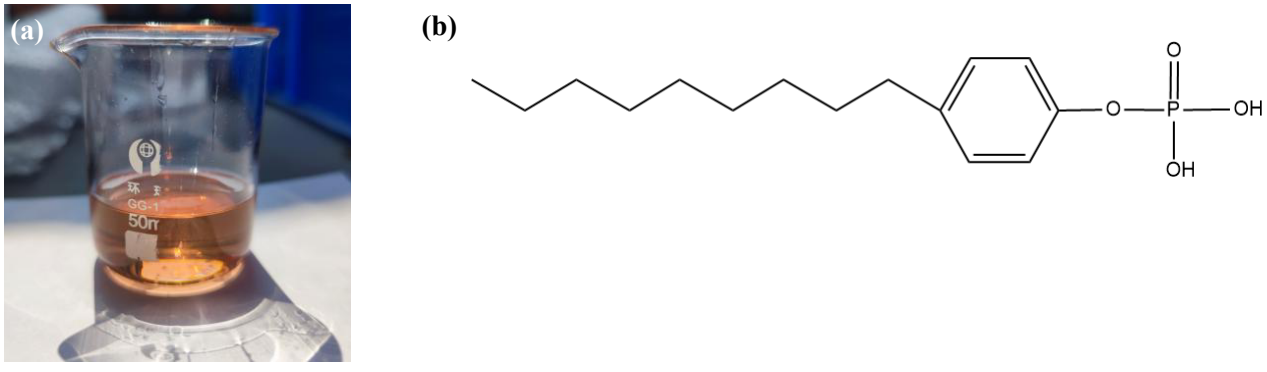

Fig. 1. The photo (a) and molecular structure (b) of NAPE

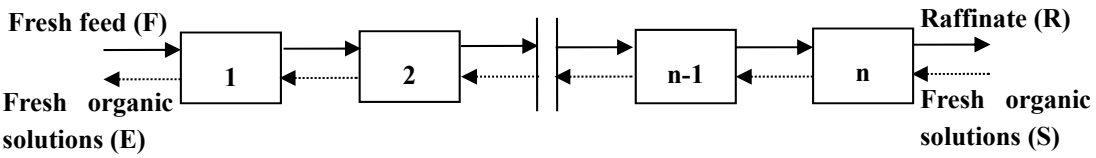

Fig. 2. The flowsheet of n-stage counter current extraction

In this study, separatory funnels were utilized to simulate cascade counter-current extraction experiments. During the experimental procedure, '*n*' separatory funnels were employed to simulate '*n*' stages of counter-current extraction. For instance, in a 5-stage (3+2) counter-current extraction, five separatory funnels were used for the simulation. The experimental procedure was presented in Fig. 3.

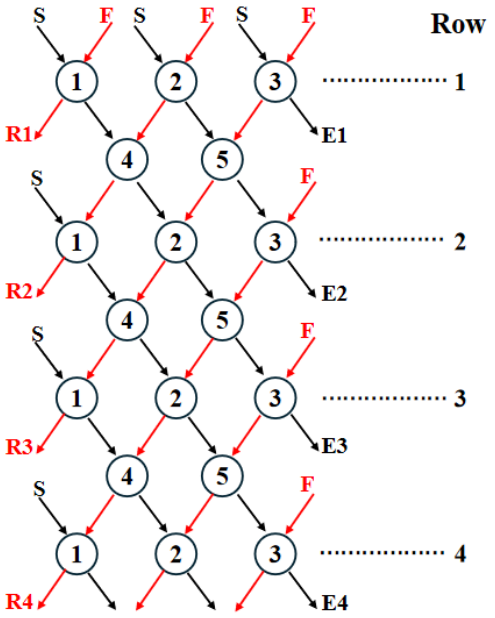

Fig. 3. Diagram of simulating *n*-stage counter-curent extraction/stripping operation with *n* separator funnel (Taking five-stage as an example)

In Fig. 3, each circle represents a single experimental contact, with the numbers inside the circles indicating the separatory funnel numbers. The numbers on the far right denote the row number. F and S stand for the fresh feed liquid and fresh organic phase, respectively, while E and R represent the loaded organic phase and raffinate, respectively. The direction of material flow is indicated by arrows. In the first row, fresh feed liquid and organic phase were added to separatory funnels 1, 2, and 3, and then shaken for a certain time in a constant temperature water bath shaker. After phase separation, the raffinate from funnel 1 was drained, and the loaded phase was transferred to the empty funnel 4. The raffinate from funnel 2 was drained into funnel 4, and the loaded phase was transferred to the empty funnel 5. The raffinate from funnel 3 was drained into funnel 5, and the loaded phase was discharged. After shaking and phase separation, funnels 4 and 5 were sequentially opened according to the arrow indications, and the loaded and raffinate phases were placed into the previous funnels 1, 2, and 3. At this point, the funnels numbered 1, 2, and 3 became the second row. The second row was then subjected to feeding, shaking, phase separation, and operation according to the arrow indications, and this process was repeated until the raffinate concentration stabilizes [51]. The simulation of counter-current stripping experiments was similar to the simulation of extraction experiments, except that the fresh feed liquid F in the extraction was replaced with the loaded organic phase E, and the fresh organic phase S was replaced with the stripping agent solution.

Samples were collected and analysed to determine the concentrations of metals therein. The aqueous samples were assayed for metals using inductively coupled plasma-atomic emission spectrometry (ICP-AES, Thermo Electron Corporation, USA). The metal concentrations of loaded organic solutions were calculated via the subtraction method.

Percentage extraction (E_1) of metals is presented in Eq. (1):

$$E_1 = 1 - \frac{[Me]_R V_R}{[Me]_F V_F} \times 100\% \quad (1)$$

Here, $[Me]_R$ and $[Me]_F$ denote the ion concentrations in the raffinate and feed liquid, respectively, measured in g/L; V_R and V_F denote the volumes of the raffinate and feed liquid, respectively, measured in mL.

Percentage stripping (E_2) of metals is presented in Eq. (2):

$$E_2 = 1 - \frac{[Me]_A V_A}{[Me]_E V_E} \times 100\% \quad (2)$$

Here, $[Me]_A$ and $[Me]_E$ denote the ion concentrations in the strip solution and the loaded organic phase, respectively, measured in g/L; V_A and V_E denote the volumes of the strip solution and the loaded organic phase, respectively, measured in mL.

3. Results and discussion

3.1. Comparison of yttrium extraction performance using P204, P507, Cyanex272 and NAPE

To compare the yttrium extraction performance of P204, P507, Cyanex272, and NAPE, an organic system comprising P204, P507, Cyanex272, or NAPE (each at 10% v/v) in sulfonated kerosene was contacted with sulfate leach solutions (at feed acidity ranging from pH 0.1 to 1.8, with an A/O ratio of 1:1, at laboratory temperature (27±1°C) for 10 minutes. The results are depicted in Fig. 4. Fig. 4 indicates that as the pH of the feed solution decreases, the extraction of yttrium by P204, P507, Cyanex272, and NAPE all diminish. When the feed pH is 1.8,

the extraction of yttrium by P204 and NAPE is high, at 97.8% and 100%, respectively, whereas the extraction by P507 is approximately 80%. As the feed pH drops from 1.8 to 0.1, the extraction by P204 and P507 plummets to below 10%. Specifically, at pH 0.5, the extraction by P507 falls to 0%, and the extraction by Cyanex272 remains between 0% and 6%. In contrast, the extraction by NAPE decreases gradually, being 76.1% at pH 0.5 and 45.6% at pH 0.1. This demonstrates that NAPE differs from P204, P507, and Cyanex272, maintaining a good extraction effect on yttrium even in a high-acid feed solution environment. Therefore, NAPE can be utilized for the direct extraction of yttrium from high-acid phosphorus ore leaching solutions.

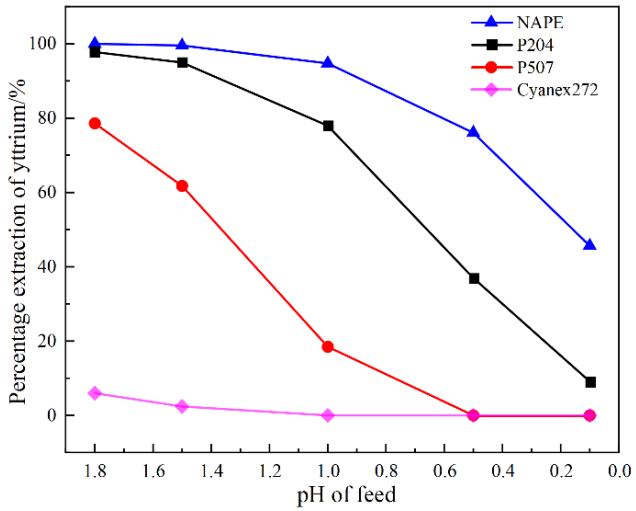

Fig. 4. Effect of pH on the extraction of yttrium using P204, P507, Cyanex272 and NAPE

The results indicated that the acidity of NAPE surpasses that of commonly used phosphate esters, including P204, P507, and Cyanex272. The extraction efficiencies of yttrium among the extractants follow this order: NAPE > P204 > P507 > Cyanex272, which aligns with their respective acidic strength order. This variance can be attributed to the molecular structures of the active components. As depicted in Fig. 5, P507, P204, and Cyanex272 are alkyl phosphate esters. Given that the alkyl group is weakly electrophilicelectron-withdrawing, the resulting alkyl phosphate

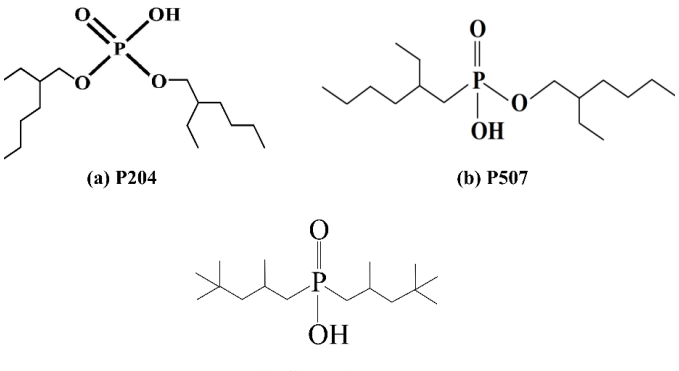

Fig. 5. Molecular structures of P204 (a), P507(b), and Cyanex272(c)

ester exhibits only mild acidity and is unable to produce H^+ ions to exchange with yttrium ions in strongly acidic sulfate solutions. In contrast to the structures of P507, P204, and Cyanex272, the additional phenyl group in NAPE introduces a conjugation effect. This conjugation effect of the phenyl group significantly enhances the electron-donating ability of the P-OH group, promoting proton dissociation and electrophilicresulting in considerably greater acidity [52]. Consequently, NAPE is anticipated to serve as an effective extractant in strongly acidic systems.

3.2. Extraction

3.2.1. Effect of feed acidity on the metal extraction

The effect of feed acidity within the pH range of 0.1 to 1.8 on metal extraction was investigated using an organic system consisting of 10% (v/v) NAPE in sulfonated kerosene and sulfate leach solutions with an A/O ratio of 1:1, at a laboratory temperature of 27±1°C for 10 minutes. The results are depicted in Fig. 6.

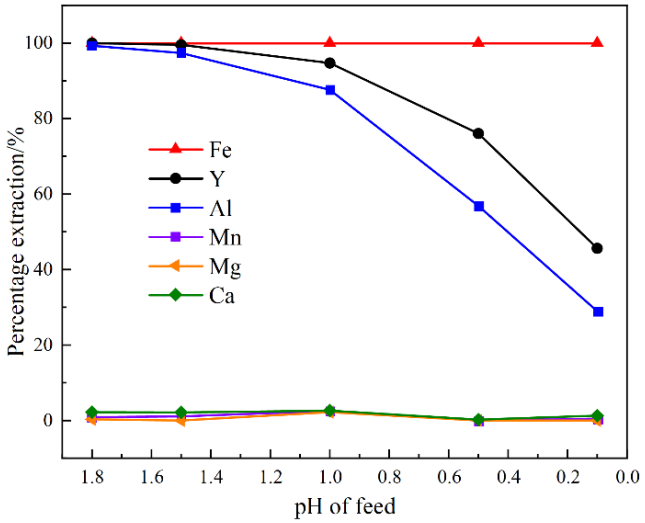

Fig. 6. Effect of pH on the extraction of different metals using NAPE as extractant

Fig. 6 illustrated that as the feed liquid pH decreased, the extraction efficiencies of yttrium and aluminum diminished. When the feed liquid pH decreased from 1.8 to 0.1, the extraction of aluminum dropped from 99.3% to 28.9%, and the extraction of yttrium decreased from 100% to 45.6%. At a feed liquid pH of 0.5, the extraction of yttrium was 76.1%. Consequently, to achieve a high yttrium extraction rate (>70%), the feed liquid pH should not be lower than 0.5. Across the entire range of feed liquid pH values, the co-extraction of iron remained nearly 100%, while the extraction of other impurity ions such as manganese, magnesium, and calcium remained consistently low (ranging from 0% to 3%) and could be considered negligible. Therefore, as long as the feed liquid pH was maintained at or above 0.5, NAPE could selectively extract and remove various impurity ions (manganese, magnesium, calcium) from the strongly acidic

phosphate ore leaching solution, while iron and aluminum were not significantly extracted. In actual high-acid phosphate ore leaching solutions (with a pH < 1), a pH range of 0.5 to 1.0 was advantageous for the extraction and separation of yttrium. Given that the extraction of impurity ions like manganese, magnesium, and calcium was negligible during the extraction process, subsequent research would concentrate on the extraction of yttrium, iron, and aluminum.

3.2.2. Effect of NAPE concentration on metal extraction

The effect of NAPE concentration on the extraction of yttrium, iron, and aluminum was investigated. The organic system, which comprised 2.5%-15% (v/v) NAPE in sulfonated kerosene, was contacted with sulfate leach solutions at an A/O ratio of 1:1. This was conducted at laboratory temperature (27±1°C) for 10 minutes. The results are depicted in Fig. 7.

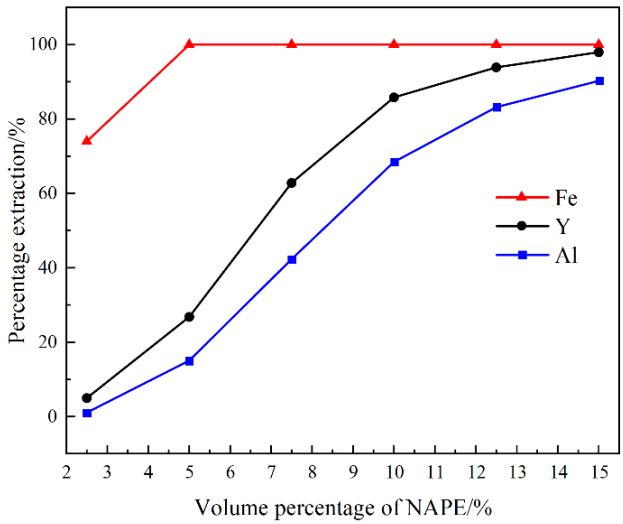

Fig. 7. Effect of the NAPE concentration on the extraction of yttrium, iron and aluminum

TABLE 2

Effect of the NAPE concentration on the extraction of phase separation time

NAPE concentration/%	2.5	5	7.5	10	12.5	15
Phase separation time/min	7	7	8	8.5	20	20

Fig. 7 illustrated that as the concentration of NAPE rose from 2.5% to 5%, iron extraction reached 100% and remained stable. When the NAPE concentration was increased from 2.5% to 10%, the extraction of yttrium and aluminum surged from 4.9% and 1.1% to 85.8% and 68.4%, respectively. However, with a further increase in NAPE concentration to 15%, the extraction of yttrium and aluminum gradually climbed to approximately 90% and 80%. Additionally, higher NAPE concentrations also elevated the viscosity of the organic phase. TABLE 2 indicated that once the extractant concentration surpassed 10%, the phase separation speed during extraction significantly decelerated. Taking all factors into account, a 10% (v/v) NAPE sulfonated kerosene organic system was chosen.

3.2.3. Effect of TBP concentration on metal extraction

The impact of TBP concentration on the extraction of yttrium, iron, and aluminum was examined. The organic system, which comprised 10% (v/v) NAPE and 0%-20% (v/v) TBP in sulfonated kerosene, was mixed with sulfate leach solutions at an A/O ratio of 1:1. This was conducted at a laboratory temperature of 27±1°C for 10 minutes. The findings are depicted in Fig. 8.

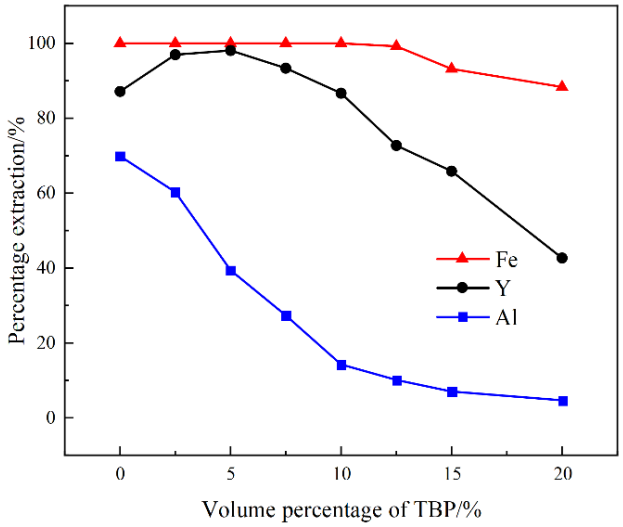

Fig. 8. Effect of the TBP concentration on the extraction of yttrium, iron and aluminium

Fig. 8 illustrated that across the entire spectrum of TBP concentrations, as the TBP concentration rose, aluminum extraction diminished from 69.9% to 4.7%. Meanwhile, iron extraction stayed close to 100% and experienced a slight decline when the TBP concentration surpassed 12.5%. As TBP concentration ascended from 0% to 5%, yttrium extraction progressively increased from 87.1% to 98.1%. Throughout the extraction process, TBP created neutral complexes with acidic phosphorus extractants and rare-earth ions, which augmented the lipophilicity of these complexes and boosted the equilibrium distribution coefficient [53]. However, with a growing volume fraction of TBP, the molecules of TBP coordinated with the complexes to form macromolecules. The high electron density on the P = O bond promoted protonation and hydrogen-bond formation, which enhanced the solubility of the complexes but concurrently suppressed the extractant's performance [54]. As TBP concentration further escalated to 20%, yttrium extraction consistently dropped to 42.7%. This indicated that a small quantity of TBP might have improved yttrium extraction through synergistic effects with NAPE, yet an excessive amount could have impeded the extraction equilibrium of yttrium. Consequently,

to guarantee a high extraction of yttrium, this study opted for an organic system comprising 10% (v/v) NAPE and 5% (v/v) TBP in sulfonated kerosene.

3.2.4. Yttrium extraction distribution isotherms and counter current extraction test

The yttrium extraction distribution isotherm was determined with sulphate leach solutions with pH = 0.33 containing 0.203 g/L yttrium and organic system consisting of 10% (v/v) NAPE and 5% (v/v) TBP in sulfonated kerosene using A/O ratios of 5:1, 3:1, 2:1 and 1:1 at the laboratory temperature (27±1°C) for 10 min (Fig. 9). As shown in the McCabe-Thiele diagram constructed for the sulphate leach solutions, five stages are theoretically required to extract almost all the yttrium with an A/O ratio of 2:1.

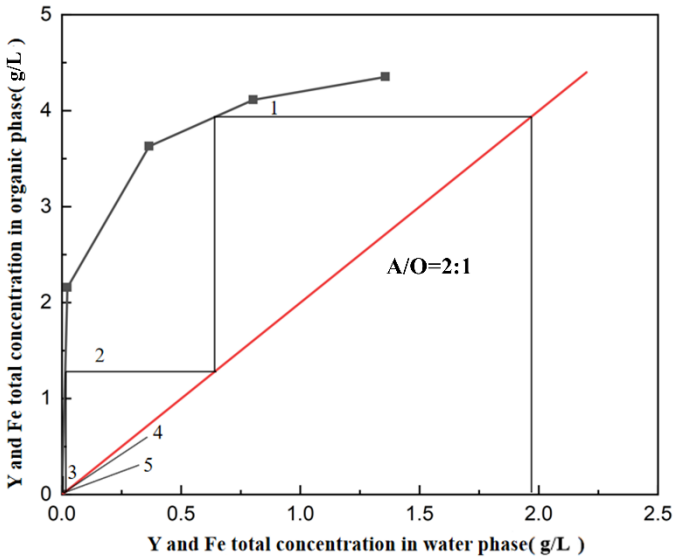

Fig. 9. McCabe-Thiele diagram for yttrium and iron extraction with the organic system consisting of 10% (v/v) NAPE and 5% (v/v) TBP in sulfonated kerosene at laboratory temperature (27±1°C)

A five-stage counter-current extraction test was conducted using an organic system comprised of 10% (v/v) NAPE and 5% (v/v) TBP in sulfonated kerosene, along with sulfate leach solutions. The test was performed at a laboratory temperature of 27±1°C with an A/O ratio of 2:1 for 10 minutes. The results, as presented in TABLE 3, indicate that 100% of the yttrium was extracted, while iron was extracted at 100%, aluminum at 4.9%, calcium at 0.49%, and neither magnesium nor manganese were extracted. Evidently, yttrium was separated from other metals in the sulfate leach solutions, except for iron, using the NAPE extractant system. Considering the low concentrations of aluminum and calcium in the feed liquid, they will not be taken into account in the subsequent stripping process. Other impurity ions remained largely unextracted. The concentrations of yttrium and iron in the loaded organic solutions were determined by the subtraction method to be 0.406 g/L and 3.5 g/L, respectively.

TABLE 3

Test results of the five-stage counter current extraction

Element	Y	Fe	Al	Ca	Mg	Mn
Feed (g/L)	0.203	1.75	0.830	0.670	5.40	0.501
Raffinate (g/L)	0	0	0.7897	0.6667	5.40	0.501
Percentage extraction (%)	100	100	4.9	0.49	0	0
Loaded organic solutions (g/L)	0.406	3.5	0.0806	0.0066	0	0

3.3. Stripping

3.3.1. Effect of H_2SO_4, HCl, HNO_3 and $H_2C_2O_4$ concentrations on the stripping of yttrium and iron

After extraction, the appropriate stripping reagent was selected by sequentially stripping the loaded organic solution with H_2SO_4 solutions (concentrations ranging from 0.5 to 6.0 mol/L), HCl solutions (concentrations ranging from 0.5 to 6.0 mol/L), HNO_3 solutions (concentrations ranging from 0.5 to 6.0 mol/L), and $H_2C_2O_4$ solutions (concentrations ranging from 0.1 to 1.0 mol/L), all at an A/O ratio of 1:1 and a laboratory temperature of 27±1°C for 10 minutes. The results are depicted in Fig. 10.

Figs. 10(a), 10(b), and 10(c) indicated that as the concentrations of sulfuric acid, hydrochloric acid, and nitric acid increased, the stripping of yttrium and iron showed an increase trend. A higher yttrium stripping efficiency could be attained while maintaining low iron stripping at 1 mol/L sulfuric acid, 1.5 mol/L hydrochloric acid, and 6 mol/L nitric acid. Considering both separation efficiency and economic cost, 1 mol/L sulfuric acid was selected as the first-stage stripper for the selective stripping of yttrium. Fig. 10(d) showed that as the concentration of oxalic acid increased, the stripping of iron also increased, reaching 86.6% at 1 mol/L. Since yttrium did not need to be considered in the second stage of stripping, 1 mol/L oxalic acid was chosen as the second-stage stripper for the selective stripping of iron.

3.3.2. Yttrium stripping distribution isotherms and counter current stripping test

The yttrium stripping distribution isotherm was determined using loaded organic solutions and a yttrium strip solution containing 1 mol/L H_2SO_4, with A/O ratios of 1:1, 1:2, 1:5, and 1:10, at a laboratory temperature of 27±1°C for 10 minutes (Fig. 11). As depicted in the constructed McCabe-Thiele diagram, five stages are theoretically required to strip nearly all the yttrium with an A/O ratio of 1:4.

Next, a five-stage counter-current stripping test was conducted using the loaded organic solutions and a yttrium strip solution consisting of 1 mol/L H_2SO_4 with an A/O ratio of 1:4 at a laboratory temperature of 27±1°C for 10 minutes. The results are presented in TABLE 4. The stripping efficiency for yttrium reached 97.7%, yielding a concentration of 1.5863 g/L

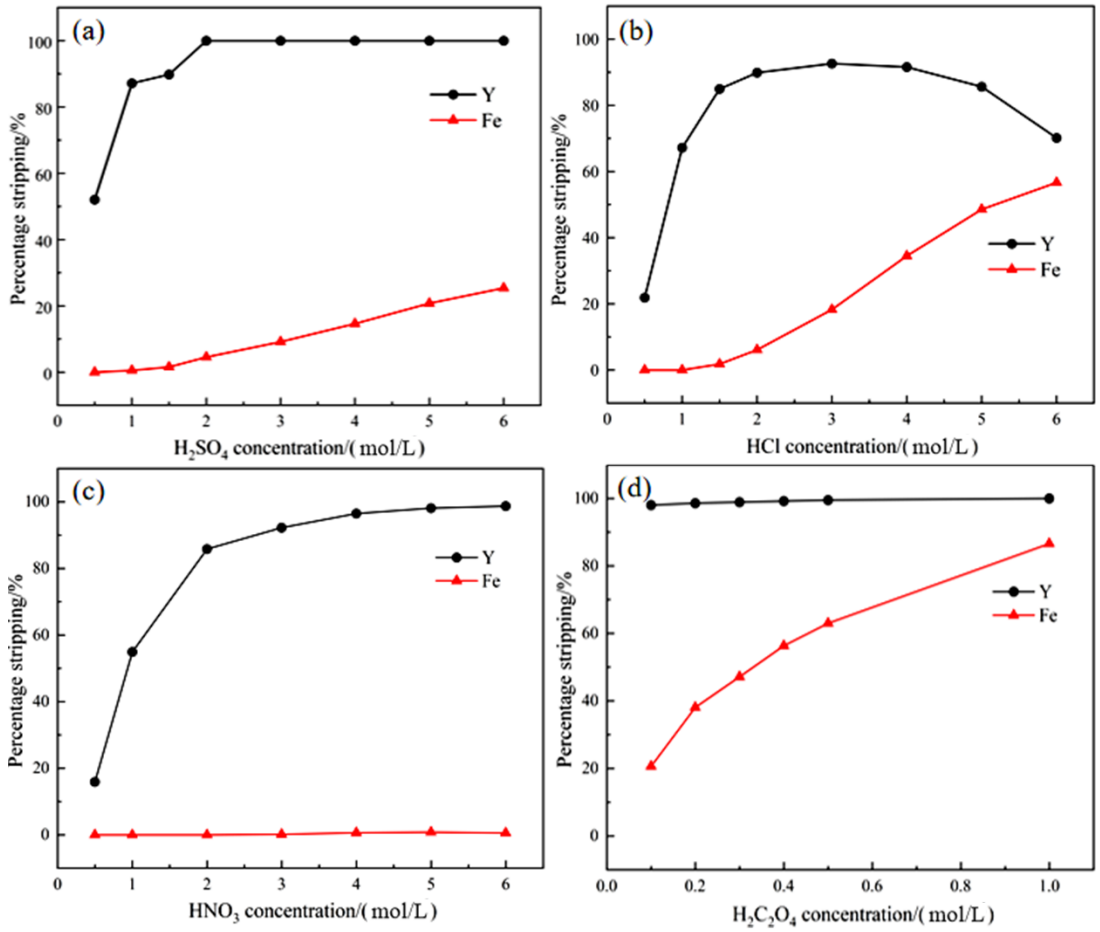

Fig. 10. Effect of (a)H_2SO_4, (b)HCl, (c)HNO_3 and (d)$H_2C_2O_4$ on the stripping of yttrium and iron

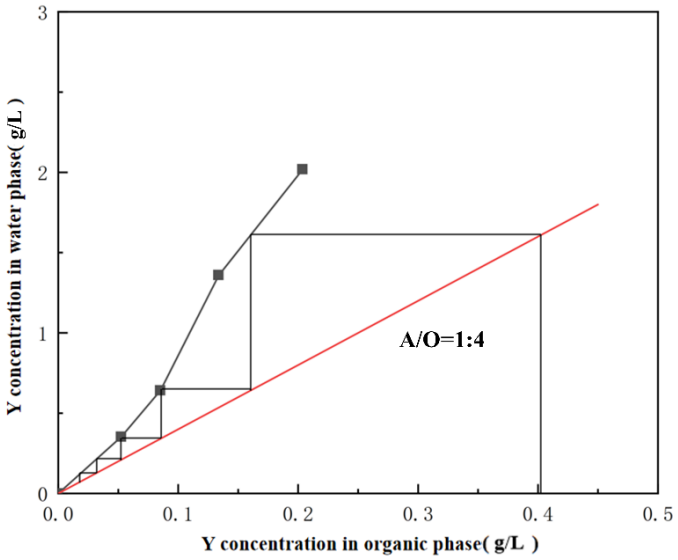

Fig. 11. McCabe-Thiele diagram for using a yttrium strip solution containing 1 mol/L H_2SO_4 at laboratory temperature (27±1°C)

of yttrium in the loaded strip liquor. In contrast, only 3.2% of the co-extracted iron was stripped, indicating that iron remained predominantly in the loaded organic solutions. Additionally, minor amounts of co-extracted aluminum and calcium were completely stripped.

TABLE 4

Test results of the five-stage counter current stripping of yttrium

Element	Y	Fe	Al	Ca
Loaded organic solutions (g/L)	0.406	3.5	0.0806	0.0066
Yttrium stripped solutions (g/L)	1.5863	0.4536	0.3224	0.0264
Percentage stripping (%)	97.7	3.2	100	100
Organic solutions after yttrium stripping (g/L)	0.0094	3.3866	0	0

3.3.3. Iron stripping distribution isotherms and counter current stripping test

The iron stripping distribution isotherm was determined using loaded organic solutions after yttrium stripping and an iron strip solution containing 1 mol/L $H_2C_2O_4$, employing A/O ratios of 1:1, 1:2, 1:5, and 1:10 at a laboratory temperature of 27±1°C for 10 minutes (Fig. 12). Based on the constructed McCabe-Thiele diagram, it was theoretically determined that five stages were required to strip nearly all the iron with an A/O ratio of 1:2.

A five-stage counter-current stripping test was conducted using loaded organic solutions following yttrium stripping and employing an iron stripping solution with a concentration of 1 mol/L $H_2C_2O_4$ at an A/O ratio of 1:2. The test was performed at a laboratory temperature of 27±1°C over a duration

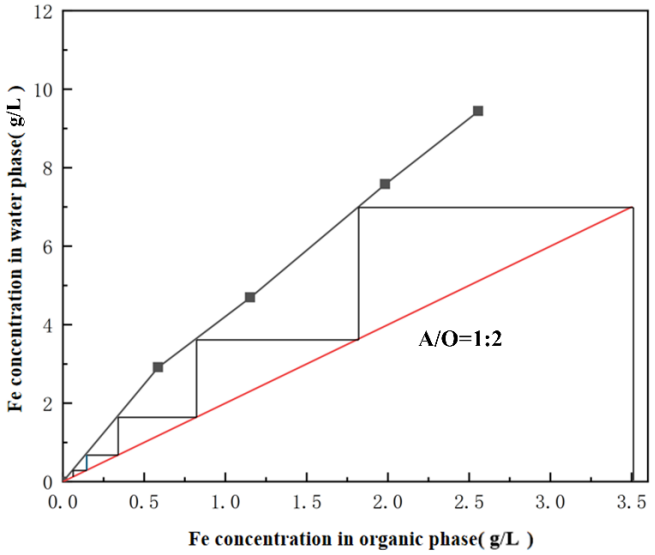

Fig. 12. McCabe-Thiele diagram for using a iron strip solution containing 1 mol/L $H_2C_2O_4$ at laboratory temperature (27±1°C)

of 10 minutes. The results indicated that 98.3% of the material was stripped. Following the iron stripping process, the extractant was washed with deionized water and subsequently regenerated for reuse.

3.4. Recovery of yttrium from stripped solutions

The yttrium in the stripped solutions was easily recovered be $Na_2C_2O_4$ precipitation. After washing, drying, and roasting the precipitate, the yttrium oxide product (Fig. 13) was obtained. The samples were subjected to ICP-AES and ICP-MS analysis, and the results were shown in TABLE 5 and TABLE 6 respectively. The results indicate that the content of major non-rare earth impurities such as Fe, Al, Mn, Mg, Ca, and P is less than 0.02%. The composition of rare earth in oxide of Y is shown in TABLE 5. It shows that the purity of Y_2O_3/REO is 89.06%.

TABLE 5

Main contents of the yttrium oxide product

Element	Fe	Al	Ca	Mg	Mn	P
Yttrium oxide product (wt.%)	0.007	0.002	0.004	<0.001	<0.001	<0.001

3.5. Process flowsheet and calculation

In industrial phosphoric ore leaching, a high-acid leach is required, producing a leachate with low pH (pH < 1) and high phosphate concentration. Conventional extractants such as P204, P507 and Cyanex272 operate outside the applicable pH range, and neutralizing the leachate prior to rare-earth recovery readily causes localized over-alkalinization, reprecipitating rare earths and iron as phosphates. Therefore, a new rare-earth recovery process employing NAPE was investigated. The process flowsheet and main inputs and outputs are presented in Fig. 14 and TABLE 7, respectively. The Effect of cycle number on the yttrium extraction is shown in Fig. 15. NAPE is recyclable and extraction capacity decreases slightly.

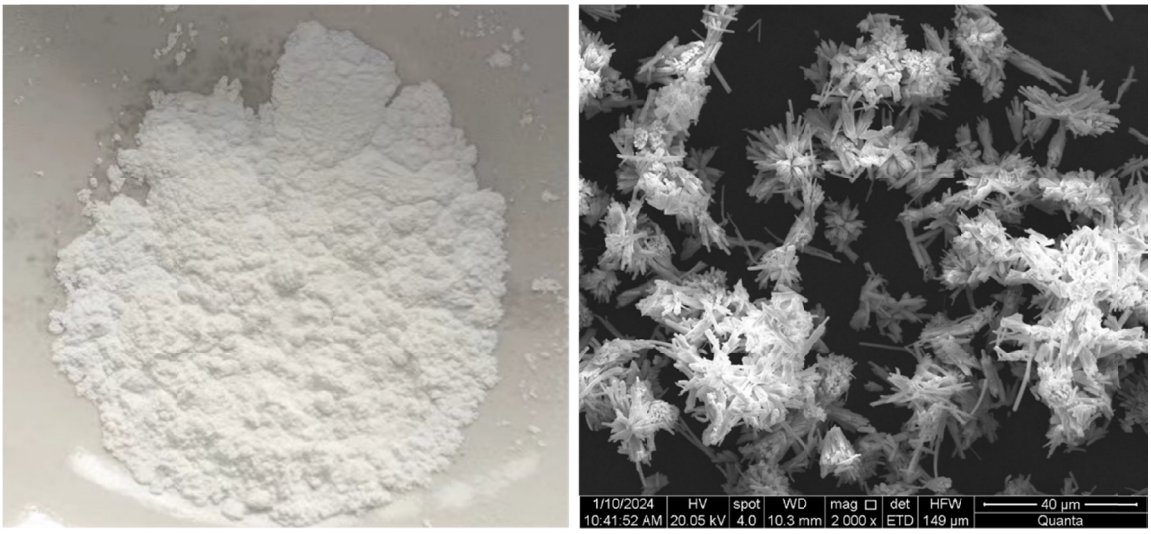

Fig. 13. SEM-mapping images of the yttrium oxide product

TABLE 6

Composition of rare earth in oxide of Y

Element	La_2O_3	CeO_2	Pr_6O_{11}	Nd_2O_3	Sm_2O_3	Eu_2O_3	Gd_2O_3	Tb_4O_7	Dy_2O_3	Ho_2O_3	Er_2O_3	Tm_2O_3	Yb_2O_3	Lu_2O_3	Y_2O_3
Content (wt.%)	0.13	0.19	<0.1	0.15	0.12	<0.1	2.03	1.32	3.76	1.05	1.21	0.24	0.47	0.15	89.06

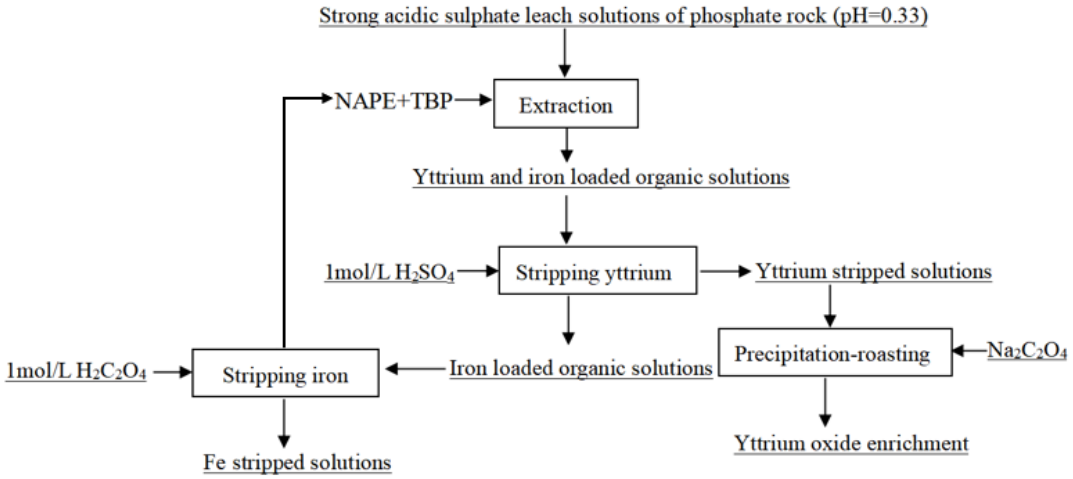

Fig. 14. Process flowsheet of yttrium recovery from strong acidic sulphate leach solutions of phosphate rock using NAPE

TABLE 7

Main inputs and outputs (based on processing one tonne of sulphate leach solutions of phosphate rock)

		Mass/g
Inputs	H_2SO_4	12500
	$H_2C_2O_4 \cdot 2H_2O$	31500
	$Na_2C_2O_4$	448
Outputs	Y_2O_3	252

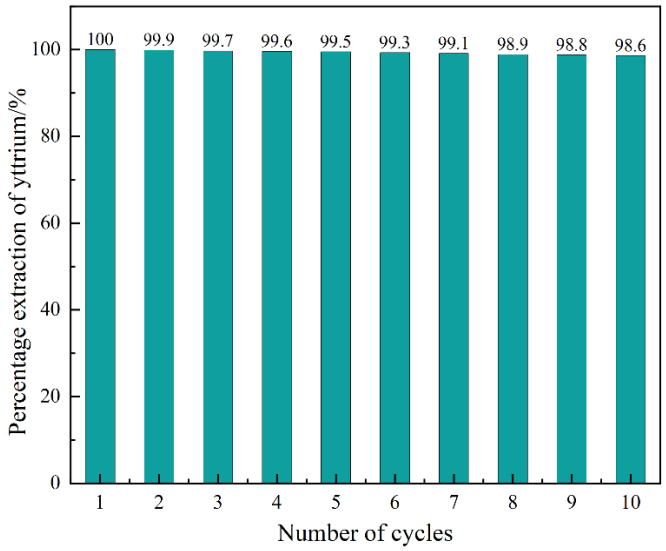

Fig. 15. Effect of cycle number on the yttrium extraction using NAPE

4. Conclusion

1) The application acidity of NAPE exceeded those of the commonly used phosphate esters (P204, P507 and Cyanex272), and could directly extract yttrium from the strong acidic sulphate leach solutions (pH = 0.33).
2) Employing a 10% (v/v) NAPE and 5% (v/v) TBP mixture in sulfonated kerosene as the extraction system, 100% of yttrium was extracted from sulfuric solutions with a pH of 0.33 and a yttrium concentration of 0.203 g/L through a five-stage counter-current extraction process. This was achieved using an organic system composed of 10% (v/v) NAPE and 5% (v/v) TBP in sulfonated kerosene with an A/O ratio of 2:1, at a laboratory temperature of 27±1°C over 10 minutes. Concurrently, the extraction of other metals such as aluminum, magnesium, manganese, and calcium was minimal, with the exception of iron. Subsequently, 97.7% of the yttrium in the loaded organic phase was selectively stripped using a 1 mol/L H_2SO_4 solution through a five-stage counter-current stripping process with an A/O ratio of 1:4 at 27±1°C over 10 minutes, followed by the use of a 1 mol/L $H_2C_2O_4$ solution to strip the co-extracted iron for recycling purposes. Throughout the entire process, 97.7% of yttrium was recovered and concentrated in the pure yttrium sulfate strip liquor, achieving a concentration of 1.5863 g/L.
3) The yttrium in the stripped solutions was easily precipitated using sodium oxalate. After roasting, a yttrium oxide product was obtained with impurity elements such as Fe, Al, Mn, Mg, Ca, and P content less than 0.02%.

Acknowledgments

This study was funded by the National Natural Science Foundation of China (No. 52374354), GanPo Yingcai Support Program. Youth Innovative Leading Talent Support Project (No. gpyc20240040), Ganpo Juncai Support Program. Youth Science and Technology Talent Support Project (2025QT15), Ganzhou Key Laboratory project (2024YSPT0001) and Startup Foundation for Doctor Talents of Gannan University of Science and Technology.

REFERENCES

[1] R. Shu, Z. Yang, Y. Cao, Z. Li, Y. Chen, H. Wang, Effect of rare earth Y on microstructure and properties of H13 steel. Heat. Treat. Met. **48** (5), 70-77 (2023).
DOI: https://doi.org/10.13251/j.issn.0254-6051.2023.05.012

[2] G. Xu, J. Luo, X. Wan, Y. Li, X. Xiong, H. Teng, Y. Gao, Study on diffusion bonding technology of yttrium target and copper alloy backingplate. Chin. Rare Earths. **44** (2), 71-76 (2023). DOI: https://doi.org/10.16533/j.cnki.15-1099/tf.202302008

[3] B. Han, X. Tian, P. Lu, X. Qi, Effects of Y_2O_3 on pack boronizing of TC4 titanium alloy. Surf. Technol. **52** (8), 451-457 (2023). DOI: https://doi.org/10.16490/j.cnki.issn.1001-3660.2023.08.041

[4] X. Li, S. Zhang, Z. Wang, Y. Guo, X. Lu, Effect of rare earth Y_2O_3 on the microstructure and properties of AZ31B magnesium alloy coatings prepared by micro-arc oxidation. Mater. Prot. **55** (10), 37-42 (2022). DOI: https://doi.org/10.16577/j.issn.1001-1560.2022.0273

[5] M. Hu, H. Yang, X. Luo, L. Wen, M. Hu, Effect of yttrium doping on microstructure and mechanical properties of CoCrFeNi high entropy alloy prepared by molten salt electrolysis. Iron Steel Vanadium Titanium. **46** (3), 174-179 (2025). DOI: https://doi.org/ 10.7513/j.issn.1004-7638.2025.03.024

[6] L. Tang, Construction and energy transfer mechanism of high-performance YVO_4-based rare earth hybrid luminescent materials. New Chem. Mater. **24** (3), 1-7 (2024). DOI: https://doi.org/10.19817/j.cnki.issn1006-3536.2024.07.044

[7] Y. Zhang, C. Wang, F. Li, Y. Zhu, S. Ma, Preparation and characterization of Y_2O_3: Eu^{3+} and Y_2O_3-SiO_2: Eu^{3+} Materials. Chem. World. **63** (6), 388-392 (2022). DOI: https://doi.org/10.19500/j.cnki.0367-6358.20210308

[8] N. Li, C. Xin, Y. Fang, J. Fan, Z. Yang, Preparation of samarium yttrium codoped fluorescent complexes and its application in potential fingerprint appearance. Shandong Chem. Ind. **52** (12), 26-28 (2023). DOI: https://doi.org/10.19319/j.cnki.issn.1008-021x.2023.12.028

[9] H. Peng, H. Zeng, Y. Wang, H. Zeng, F. Liu, J. Huang, Synthesis and optical property of Dy^{3+}-doped vanadium-phosphate yttrium nanomaterials. New Chem. Mater. **50** (11), 116-120 (2022). DOI: https://doi.org/10.19817/j.cnki.issn1006-3536.2022.11.023

[10] X. Ye, A. Xie, Preparation and luminescence properties of Eu^{3+} doped yttrium tungstate phosphors. J. Xiamen Univ. Technol. **30** (01), 58-64 (2022). DOI: https://doi.org/10.19697/j.cnki.1673-4432.202201009

[11] Z. Li, J. Zhao, Q. Li, C. Li, W. Cai, J. Chang, W. Yang, Effect of neodymium-doped yttrium aluminum garnet laser combined with desensitizing toothpaste on dentinal tubule occlusion against acid challenge. Acta. Acad. Med. Sin. **45** (5), 809-813 (2023). DOI: https://doi.org/10.3881/j.issn.1000-503x.15697

[12] Y. Yang, H. Luo, C. Guo, B. Li, Z. Zhou, Preparation of Ho: BaY_2F_8 laser fluoride crystal atmosphere. Mod. Chem. Res. (4), 175-177 (2023). DOI: https://doi.org/10.20087/j.cnki.1672-8114.2023.04.056

[13] B. Shen, Z. Wang, C. Yu, X. Wang, S. Wang, L. Hu, W. Wei, Research progress of rare earth doped yttrium aluminum garnet crystal laser fiber. Mater. Rev. **35** (9), 9123-9132 (2021). DOI: https://doi.org/10.11896/cldb.19120095

[14] S. Peng, C. Cai, J. Zheng, S. Guo, Y. Xu, D. Zhou, Application of YBCO high temperature superconducting tapes in superconducting energy storage devices. J. Shanghai Univ., Nat. Sci. Ed. **28** (5), 813-820 (2022). DOI: https://doi.org/1007-2861(2022)05-0813-08

[15] Z. Xu, Y. Kong, Z. Yin, Study on high - temperature antibonding performance of load bearing boards coated with nano yttrium stabilized zirconia coating. Mater. Prot. **56** (12), 44-49+78 (2023). DOI: https://doi.org/10.16577/j.issn.1001-1560.2023.0287

[16] C. Bian, Y. Qian, G. Cui, Y. Liu, Z. Kou, Tribological properties of CoCrNiFe matrix high - temperature composite coatings reinforced by yttrium element. Mater. Rev. **36** (8), 137-143 (2022). DOI: https://doi.org/10.11896/cldb.21010202

[17] J. Wang, L. Bao, L. Chao, Study on superconductivity and optical absorption of yttrium hexaboride nanoparticles. J. Inn. Mong. Norm. Univ., Nat. Sci. Ed. **50** (3), 204-209 (2021). DOI: https://doi.org/10.3969/j.issn.1001-8735.2021.03.003

[18] S. Hu, Y. Tang, G. Zhou, S. Wang, Digital light processing 3D printing of $Y_3Al_5O_{12}$ transparent ceramics and microstructure regulation. J. Chin. Ceram. Soc. **52** (3), 882-889 (2024). DOI: https://doi.org/10.14062/j.issn.0454-5648.20230673

[19] D. Huang, Y. Niu, S. Li, Z. Dong, Z. Bao, S. Zhu, Thermal cycling and flame thermal shocking failure mechanism of tetragonal yttria - stabilized zirconia TBCs prepared on high temperature alloys by suspension plasma spraying. Chin. J. Mater. Res. **24** (3), 1-11 (2024). DOI: https://doi.org/10.11901/1005.3093.2023.471

[20] D. Wang, J. Wang, H. Yuan, Z. Liu, J. Zhou, J. Deng, X. Wang, B. Wu, J. Zhang, S. Wang, Metre-scale $Y_3Al_5O_{12}$ (YAG) transparent ceramics by vacuum reactive sintering. J. Inorg. Mater. **38** (12), 1483-1484 (2023). DOI: https://doi.org/10.15541/jim20230374

[21] A. Yan, G. Ding, S. Guo, B. Deng, R. Chen, Application of high abundance yttrium in permanent magnetic materials. J. Chin. Soc. Rare Earths. **39** (3), 425-435 (2021). DOI: https://doi.org/10.11785/s1000-4343.20210306

[22] Z. Xiao, The rare earth element yttrium and its applications. Rare Earth Inf. (8), 30-32 (2005). DOI: https://doi.org/CNKI:SUN:XTXX.0.2005-07-015

[23] J. Chen, R. Yang, J. Zhang, Occurrence of yttrium in the Zhijin phosphorus deposit in Guizhou Province, China. Open Geosci. **14** (1), 776-784 (2022). DOI: https://doi.org/10.1515/geo-2020-0297

[24] K. Zhang, Z. Liu, C. Sun, H. Cao, K. Zhu, W. Zhu, W. Li, Recovery of yttrium from deep-sea mud. J. Rare Earths. **36** (8), 863-872 (2018). DOI: https://doi.org/10.15261/serdj.29.49

[25] E. Ma, P. Jiang, P. Jin, Kinetics and mechanism of yttrium extraction with three acidic phosphorus extractants. J. Chem. Technol. Biotechnol. **51** (3), 315-321 (1991). DOI: https://doi.org/10.1002/jctb.280510304

[26] Y. He, S. Guo, M.I. Khan, K. Chen, S. Li, L. Zhang, S. Yin, Liquid - liquid extraction of yttrium (III) using 2-ethylhexyl phosphonic acid mono-2-ethylhexyl (EHEHPA) in a microreactor: a comparative study. ACS Sustain. Chem. Eng. **7** (1), 1616-1621 (2019). DOI: https://doi.org/10.1021/acssuschemeng.8b05334

[27] N. Fu, Z. Sui, M. Tanaka, Equilibrium analysis of solvent extraction of yttrium (III) and europium (III) from hydrochloric acid with P507. T. Nonferr Metal. Soc. **21** (9), 2093-2098 (2011). DOI: https://doi.org/10.1016/S1003-6326(11)60978-3

[28] X. Wang, W. Li, S. Meng, D. Li, The extraction of rare earths using mixtures of acidic phosphorus-based reagents or their thio-

analogues. J. Chem. Technol. Biotechnol. **81** (5), 761-766 (2006). DOI: https://doi.org/10.1002/jctb.1532

[29] X. Wang, W. Li, D. Li, Extraction and stripping of rare earths using mixtures of acidic phosphorus-based reagents. J. Rare Earths. **29** (5), 413-415 (2011). DOI: https://doi.org/10.1016/S1002-0721(10)60470-x

[30] Y. Xiong, W. Li, D. Wu, D. Li, S. Meng, Kinetics and mechanism of Yb(III) extraction and separation from Y(III) with mixtures of bis(2,4,4-trimethylpentyl) phosphinic acid and 2-ethylhexyl phosphonic acid mono-2-ethylhexyl ester. Sep. Sci. Technol. **41** (1), 167-178 (2006). DOI: https://doi.org/10.1080/01496390500459445

[31] M. Karve, B. Vaidy, Selective separation of scandium(III) and yttrium(III) from other rare earth elements using Cyanex302 as an extractant. Sep. Sci. Technol. **43** (5), 1111-1123 (2008). DOI: https://doi.org/10.1080/01496390801887435

[32] D. Wu, Y. Xiong, D. Li, Mass transfer kinetics of yttrium(III) using a constant interfacial cell with laminar flow. Part I. Extraction with Cyanex302. Hydrometallurgy **82** (3), 176-183 (2006). DOI: https://doi.org/10.1016/j.hydromet.2006.03.042

[33] D. F. Peppard, J. Faris, P. Gray, G. Mason, Study of the solvent extraction of the transition elements. I. Order and degree of fractionation of the trivalent rare earth. J. Phys. Chem. **57** (3), 294-301 (1953). DOI: https://doi.org/10.1021/j150504a008

[34] D. Saha, E.S. Vadivu, R. Kumar, C.R.V. Subramani, Separation of bulk Y from 89Y(n,p) produced 89Sr by extraction chromatography using TBP coated XAD-4 resin. J. Radioanal. Nucl. Chem. **298** (2), 1309-1314 (2013). DOI: https://doi.org/10.1007/s10967-014-3253-4

[35] D. Zou, Extraction-separation process for U, Fe, Th and rare earth elements in monazite. Mater. Res. Appl. **2** (1), 16-22 (1992). DOI: https://doi.org/CNKI:SUN:GDYS.0.1992-01-003

[36] K. Zhang, X. Zhong, J. Tao, R. Wang, Z. Liu, A stepwise solvent extraction process for recovering yttrium from sulphate leach solutions of deep - sea mud. Solvent Extr. Res. DEV. **29** (2), 49-59 (2022). DOI: https://doi.org/10.15261/serdj.29.49

[37] D. Chu, G. Ma, D. Li, Extraction of rare earth ions from nit medium with Cyanex923. Chin. J. Anal. Chem. **26** (11), 1346-1349 (1998). DOI: https://doi.org/10.0000/98ee4cb017cb469ba8b8759fe2d221a0

[38] W. Li, X. Wang, H. Zhang, S. Meng, D. Li, Solvent extraction of lanthanides and yttrium from nit medium with Cyanex925 in heptane. J. Chem. Technol. Bio. **82** (4), 376-381 (2007). DOI: https://doi.org/10.1002/jctb.1680

[39] X. Li, F. Li, T. Zhu, D. Wu, L. Song, Extraction and separation of rare earths using mixtures of sec-nonylphenoxy acetic acid and alkylated phosphine oxides. Chin. J. Anal. Chem. **49** (12), 49-53 (2021). DOI: https://doi.org/10.1016/j.cjac.2021.08.004

[40] Q. Han, J. Li, W. Bai, Technology optimization to sepa and purify yttrium with naphthenic acid. Mater. Res. Appl. **4** (2), 137-141 (2010). DOI: https://doi.org/10.3969/j.issn.1673-9981.2010.02.013

[41] K. Liu, Z. Wang, J. Mei, B. Lu, Y. Wu, S. Yang, X. Lin, A green yttrium extraction system containing naphthenic acid, trioctyl/decylamine and isopropanol. J. Clean. Prod. **415**, 137747 (2023). DOI: https://doi.org/10.1016/j.jclepro.2023.137747

[42] W. Li, X. Wang, S. Meng, D. Li, Y. Xiong, Extraction and separation of yttrium from the rare earths with sec-octyl phenoxy acetic acid in chloride media. Sep. Purif. Technol. **54** (2), 164-169 (2007). DOI: https://doi.org/10.1016/j.seppur.2006.08.029

[43] X. Guo, R. Yang, Y. Gong, Z. Jiang, Y. Dong, X. Sun, Insights into the coordination and extraction of yttrium(III) ions with a phenoxyacetic acid ionic-liquid extractant. Eur. J. Inorg. Chem. (17), 2332-2339 (2017). DOI: https://doi.org/10.1016/10.1002/ejic.201601491

[44] Y. Wang, Y. Xiong, S. Meng, D. Li, Separation of yttrium from heavy lanthanide by CA-100 using the complexing agent. Talanta. **63** (2), 239-243 (2004). DOI: https://doi.org/10.1016/j.talanta.2003.09.034

[45] X. Sun, Y. Wang, D. Li, Selective separation of yttrium by CA-100 in the presence of a complexing agent. J. Alloys Compd. **408-412**, 999-1002 (2006). DOI: https://doi.org/10.1016/j.jallcom.2004.12.137

[46] H. Singh, S.L. Mishra, R. Vijayalakshmi, Uranium recovery from phosphoric acid by solvent extraction using a synergistic mixture of di-nonyl phenyl phosphoric acid and tri-n-butyl phosphate. Hydrometallurgy. **73**, 63-70. (2004). DOI: https://doi.org/10.1016/j.hydromet.2003.08.006

[47] H. Singh, R. Vijayalakshmi, S.L. Mishra, C.K. Gupta, Studies on uranium extraction from phosphoric acid using di-nonyl phenyl phosphoric acid-based synergistic mixtures. Hydrometallurgy. **59**, 69-76. (2001). DOI: https://doi.org/10.1016/s0304-386x(00)00145-6

[48] R. Ma, Extraction Metallurgy, Metallurgical industry press, Beijing, PP 328-354 (2009).

[49] F. Liu, Fundamental Research of Extracting Vanadium based on Vanadium Leaching Agent and Producing High Purity V_2O_5 with Compact Process. Tianjin University (2014).

[50] J. Gao, Control of distillation - application of McCabe - Thiele diagrams. Chem. World. (11), 543-550 (1955). DOI: https://doi.org/10.19500/j.cnki.0367-6358.1955.11.022

[51] K. Zhang, Study of recovery of gallium and germanium from high concentration sulfate acid liquor by extraction. Central South University (2014).

[52] S. Li, J. Yang, H. Liu, J. Ning, B. Han, S. Yang, H. Yu, F. Hu, H. Zhang, Y. Chen, Efficient zinc extraction from industrial wastewater with novel phenyl phosphate for saline wastewater net-zero emission. Desalination. **611**, 118926 (2025). DOI: https://doi.org/10.1016/j.desal.2025.118926

[53] A. Zhang, Synergistic Extraction of RE(III) with H_2A and TBP. Chin. J. Rare Met. **25** (1), 32-35. (2001). DOI: https://doi.org/10.13373/j.cnki.cjrm.2001.01.008

[54] H. Li, D. Han, J. Zhang, X. Jiang, F. Ge, Z. Hu, Enrichment of high concentration rare earth leaching solution. Chin. Nonferrous Metall. **52** (6), 53-59. (2023). DOI: https://doi.org/10.19612/j.cnki.cn11-5066/tf.2023.06.006